Available online at www.sciencedirect.com
SCIENCE DIRECT®
ELSEVIER
Journal of Solid State Chemistry 177 (2004) 3859–3867
JOURNAL OF SOLID STATE CHEMISTRY
www.elsevier.com/locate/jssc

The reflectivity spectra of $ZnXP_2$ (X = Si, Ge, and Sn) compounds

F. Chiker[a,*], B. Abbar[a], S. Bresson[b], B. Khelifa[b], C. Mathieu[b], A. Tadjer[a]

[a]Computational Materials Science Laboratory, Département de Physique, Faculté des Sciences, Université Djillali Liabès de Sidi Bel Abbès, Algeria.
[b]Centre de Calcul et de Modélisation de Lens, Université d'Artois, Lens SP18, France

Received 5 January 2004; received in revised form 24 May 2004; accepted 13 July 2004
Available online 21 September 2004

Abstract

Full Potential Augmented Plane Wave plus local orbital method (FAPW + *lo*) calculations were performed for $ZnSiP_2$, $ZnGeP_2$, and $ZnSnP_2$ in the chalcopyrite structure in order to investigate the optical properties and to show the origin of the different optical transitions and their correspondence in the band structure. It is found that the most important features of the band gap is pseudo-direct for $ZnSiP_2$, indirect for $ZnGeP_2$, and direct for $ZnSnP_2$. Then the contribution of the different transitions peaks are analyzed from the imaginary part of the dielectric function and the reflectivity spectra.
© 2004 Elsevier Inc. All rights reserved.

Keywords: Reflectivity spectra; $ZnSiP_2$; $ZnGeP_2$; $ZnSnP_2$ semiconductors

1. Introduction

Recently, the zinc germanium diphosphide ($ZnGeP_2$) [1,2] crystallizing in the chalcopyrite structure, has been attracting interest due to its promising applications for non-linear optical parametric oscillator laser systems in the mid-infrared. It can provide continuous laser output over the range from 3 to 8 μm at conversion efficiency above 50% when used as an optical parametric oscillator pumped at 2 μm. It shows a large nonlinear optical coefficient an appropriate birefringence, a wide range of transparency [3], and high thermal conductivity, which are suitable for its applications. However, there is a broad optical absorption around 1 μm limiting the performance of optical parametric oscillator. Also $ZnSnP_2$ has received a great deal of attention as a photovoltaic material, it is a potentially interesting photovoltaic material which is composed of relatively abundant elements [4–8].

Nowadays the standard tool of theoretical condensed matter physics to deal with the electronic and lattice properties of solids is density functional theory (DFT), on the basis of the works of Hohenberg–Kohn [10] and Kohn–Sham [9]. This extremely successful and simple theory, which was established almost 40 years ago has been immensely popular, first in physics and chemistry and for last 10 years also for biology. DFT, in its many forms helped in understanding many different properties of systems as simple as atoms to very complicated surface structures. In condensed matter applications, it is generally used within so called local density approximation (LDA), which has been used successfully to compute the excited states, namely, optical and magneto-optical properties, X-ray absorption spectra. It is then crucial to use a good basis-set for the description of the electronic structure of realistic systems. The augmented plane wave (APW) [11], Korringa–Khon–Rostoker (KKR) [12], and linear muffin-tin orbital (LMTO) [13] methods can be used, in principle, to solve exactly the Khon–Sham equations. In this paper we will use the new Full Potential Augmented Plane Wave plus local orbital method (FAPW + *lo*) [14,15] to study excited states of the $ZnSiP_2$, $ZnGeP_2$, and $ZnSnP_2$ ternary Pnictide semiconductors [18–29] within a LDA.

This paper, which is far from being a review paper about calculated excited states, tries to bridge the

*Corresponding author. Fax: +213-048569546.
E-mail address: chikersba@yahoo.fr (F. Chiker).

0022-4596/$ - see front matter © 2004 Elsevier Inc. All rights reserved.
doi:10.1016/j.jssc.2004.07.020

different optical transitions between the reflectivity spectra and their correspondence in the band structure of three ternary Pnictide semiconductors in the chalcopyrite structure. In the first part of this paper, we describe the construction of the APW + *lo* basis set within an all- electron full potential approach which will be used to determine the momentum matrix elements. We devote the second part to the application section where we present our calculated electronic band structure of $ZnXP_2$ (with X = Si, Ge, and Sn), followed with the detailed discussion of the optical properties. Finally, our conclusions are presented in Section 4.

2. Calculation methodology

In our study of the excited states of the $ZnXP_2$ (X = Si, Ge, Sn) semiconductors, we used the new Full Potential Augmented Plane Wave method [14] of the density functional theory [9,10], and for the exchange and correlation potential we have chosen to use the LDA parameterised by Perdew and Wang [17]. Recently, the development of the Augmented Plane Wave (APW) methods from Slater's APW to LAPW and the new APW + *lo* was described by Schwarz et al. and Sjöstedt et al. [14–16].

Since, basis functions, electron densities, and potentials were expanded in combinations of spherical harmonic functions with a cut-off $l_{max} = 10$ inside spheres surrounding the atomic sites, muffin tin spheres, and in the interstitial region we used 2201, 2273, and 2599 plane waves for all $ZnSiP_2$, $ZnGeP_2$, and $ZnSnP_2$ respectively. In the calculation reported here, we made use of core state [Ar] for Zn, [Ne] for both Si and P, and [Kr] for Sn which they are treated self-consistently and fully relativistically, while the remaining valence states are treated self-consistently within the semi relativistic approximation neglecting spin–orbit correction. For sampling the irreducible edge of the Brillouin zone we have used seven special K-points in the electronic properties calculations and 401 special K-points in the optical properties treatment. Then, we have used the energy cutoff of $R_{mt}K_{max} = 8$ and the maximal reciprocal vector equal to 10. Since, the muffin-tin radii of each compound chosen in our calculation are presented in Table 1.

Table 1
The muffin-tin radius (in a.u.) chosen in our calculation treatment

	R_{mt} (Zn)	R_{mt} (X)			R_{mt} (P)
		X = Si	X = Ge	X = Sn	
$ZnSiP_2$	2.3	2.1	—	—	2.5
$ZnGeP_2$	2.2	—	2.3	—	2
$ZnSnP_2$	2.4	—	—	2.6	2

3. Results and discussion

3.1. Electronic properties

The chalcopyrite structure is a ternary analogue of the diamond structure and a superstructure of Zinc Blende. Going from binary compounds to their ternary analogues one can observe large increase of number of electronic and optical properties, which are valuable for different applications. Therefore, it is natural to compare the electronic properties of ternary chalcopyrite to their analogues. In this work, the band structure properties of $ZnXP_2$ (with X = Si, Ge, and Sn) were calculated in the chalcopyrite structure compared to their Zinc Blende binary analogues.

Since qualitatively, the band structure fall into two distinct classes corresponding to ternary compounds for which the binary analogues have direct or indirect band gaps, respectively. Figs. 1b, 2b and 3b represent the

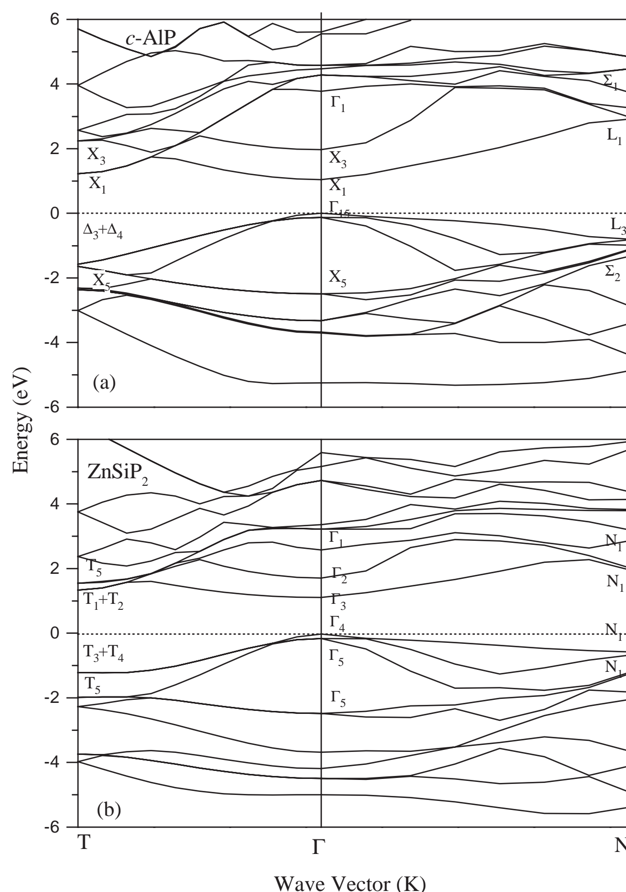

Fig. 1. Electronic band structures in the three standard energy points T, Γ, and N of the chalcopyrite Brillouin zone for $ZnSiP_2$ semiconductor (b), and its binary Zinc Blende analogue c-AlP (a).

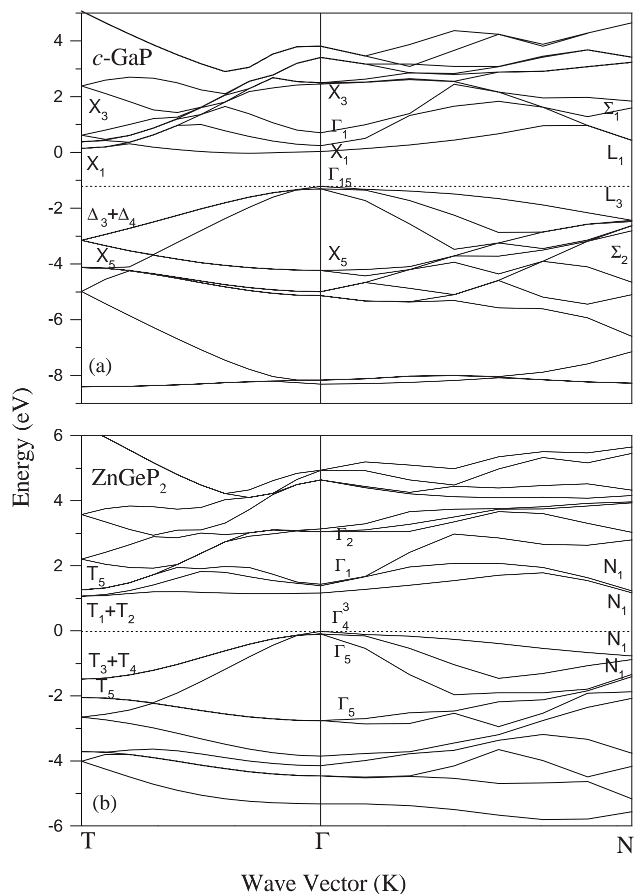

Fig. 2. Electronic band structures in the three standard energy points T, Γ, and N of the chalcopyrite Brillouin zone for $ZnGeP_2$ semiconductor (b), and its binary Zinc Blende analogue c-GaP (a).

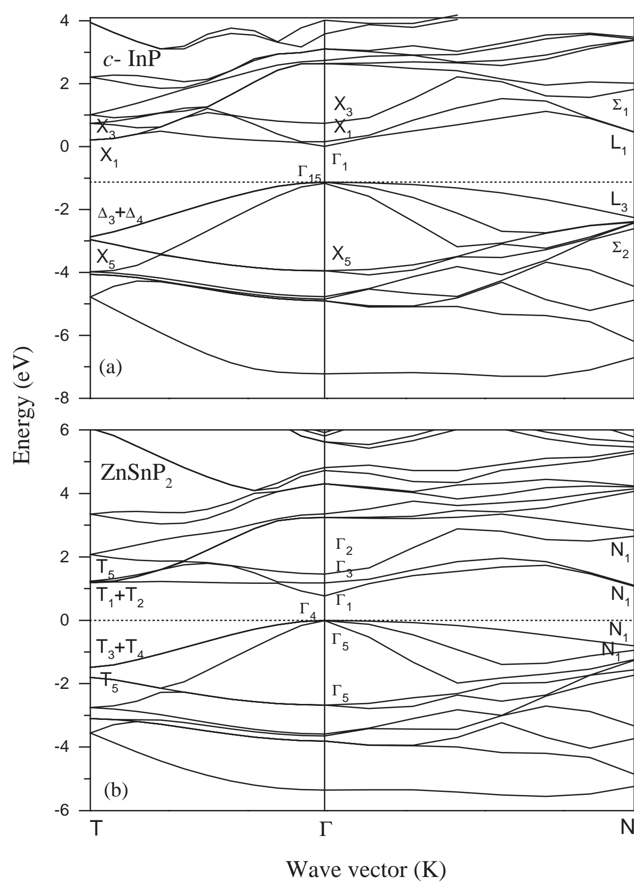

Fig. 3. Electronic band structures in the three standard energy points T, Γ, and N of the chalcopyrite Brillouin zone for $ZnSnP_2$ semiconductor (b), and its binary Zinc Blende analogue c-InP (a).

electronic band structures of $ZnSiP_2$, $ZnGeP_2$, and $ZnSnP_2$ compounds compared to their Zinc Blende AlP, GaP, and InP binary analogues respectively. Firstly, the band structure of $ZnSiP_2$ (Fig. 1b) is especially interesting because it shows a direct energy gap (at $\Gamma_{4v} \rightarrow \Gamma_{3c}$) whereas its c-AlP binary analogue [30] has an indirect energy gap ($\Gamma_{15v} \rightarrow X_{1c}$), this direct energy gap has been designated as pseudo-direct, this means that the gap is nominally direct but corresponds to weak, almost forbidden optical transition, in contrast to Shay and Tell studies [33] who found that this material has a direct band gap.

Then for $ZnGeP_2$ (Fig. 2b) there are some remaining open questions about its electronic band structure. Most notably, there has been a long-standing controversy over the nature of the band gap. From the first local density functional calculations that they performed, Jaffe and Zunger [34] obtained a pseudo-direct gap (at $\Gamma_{4v} \rightarrow \Gamma_{3c}$), followed by minima at N and T, and the empirical pseudo-potential calculations of Varea De Alvarez and Cohen [35,36] found a direct gap (at $\Gamma_{4v} \rightarrow \Gamma_{1c}$) closely followed by an indirect gap at N. More recently, some preliminary results were first reported by Zapol et al. [38] which performed all electron calculations using a Gaussian Orbital basis set and found the minimum location to depend sensitively on the unit cell volume, he obtains the order N_1, $\Gamma_1, T_1 + T_2$.

While, the calculations of Rashkeev et al. [2], using the first principles Linear Muffin-Tin Orbitals (LMTO) method within the Atomic Sphere Approximation, showed that the nature gap of $ZnGeP_2$ is indirect with a conduction-band minimum location at a point near to the N point. Then, Limpijumnong et al. [37] found several close lying conduction band minima of which the lowest one is at a low symmetry point of the Brillouin zone, and they showed that their results may account for the available experimental data and point out some problems with the traditional pseudo-direct gap interpretation. Our calculated electronic band structure of this material showed that the $ZnGeP_2$ has a valence-band maximum location at a Γ point and a conduction-band minimum location at T point, therefore we can say that this compound has an indirect band gap at T-point ($\Gamma_{4v} \rightarrow T_{1c} + T_{2c}$) like as its c-GaP binary analogue [30] which has an indirect energy gap at X-point

($\Gamma_{15v} \to X_{1c}$). Then for the latter material $ZnSnP_2$ (Fig. 3b), we have shown that its electronic band structure shows a direct band gap ($\Gamma_{4v} \to \Gamma_{1c}$) at a lower unoccupied conduction band Γ_1 like as in its *c*-InP binary analogue [30], which has a direct energy gap at Γ-point ($\Gamma_{15v} \to \Gamma_{1c}$).

Table 2 provides the correspondence between the states in chalcopyrite notation and the states in Zinc Blende. Since the triple degeneracy of the valence band in *ZB*-binary compound (Γ_{15v}) is lifted in ternary such that a non degenerate level Γ_{4v} lies above a doubly degenerate level Γ_{5v}. The higher conduction band minima Γ_{1c} is derived from Γ_{1c}. Then $T_{1c}+T_{2c}$, and Γ_{3c} conduction bands are derived from X_{1c}. Finally, Γ_{2c} is derived from X_{3c}. Table 3 presents our calculated, experimental [24], and theoretical [2,27] band gap energies. All different theoretical band gap energies data (PVMB [27]: 1.11 eV for $ZnSiP_2$, 0.61 eV for $ZnSnP_2$; LDA-LMTO [2]: 1.22 eV for $ZnSiP_2$, 1.16 for $ZnGeP_2$) agree with our band gap energies 1.135 eV for $ZnSiP_2$, 1.079 eV for $ZnGeP_2$, and 0.776 for $ZnSnP_2$ respectively.

Although all of the LDA gaps calculated using both FPLAPW and LMTO methods (see Table 3) are lower than the experimental results [24] (2.07, 2.34, and 1.66 eV for $ZnSiP_2$, $ZnGeP_2$, and $ZnSnP_2$, respectively) by approximately 1 eV. This situation is caused by the errors of the LDA calculation, which is well known that LDA often underestimates band gaps by as much as 50%.

3.2. Optical properties

The linear response of a system due to an external electromagnetic field with a small wave vector can be described with the complex dielectric function which is calculated for frequencies well above those of the phonons, and, therefore, we considered only electronic excitations. The interband contribution to the imaginary part of the dielectric function $\varepsilon_2(\omega)$ is calculated by summing transitions from occupied to unoccupied states (with fixed k vector) over the Brillouin zone, weighted with appropriate matrix element giving the probability for transition. To be specific, the components of $\varepsilon_2(\omega)$

Table 2
Selected conduction and valence band eigenvalues measured from the valence band maximum in ternary compounds and their binary analogues

Zinc blende				Chalcopyrite			
	c-AlP	*c*-GaP	*c*-InP		$ZnSiP_2$	$ZnGeP_2$	$ZnSnP_2$
Γ_{1c}	1.041	0.037	0.154	Γ_{1c}	1.104	1.163	1.180
X_{1c}	1.971	0.241	0.741	Γ_{3c}	1.702	1.383	1.455
X_{1c}	3.774	0.701	0.011	$T_{1c}+T_{2c}$	2.579	1.428	0.769
X_{3c}	1.22	0.143	0.206	Γ_{2c}	1.335	1.065	1.186
L_{1c}	2.929	0.433	0.460	N_{1c}	1.928	1.171	1.069
Γ_{15v}	0.00	−1.217	−1.127	Γ_{4v}	−0.03	−0.014	−0.007
				Γ_{5v}	−0.165	−0.095	−0.009

Table 3
Calculated largest band gaps in the valence band, heteropolar and optical gaps for $ZnSiP_2$, $ZnGeP_2$, and $ZnSnP_2$ (the results are given in eV)

	$ZnSiP_2$ (*PD*)	$ZnGeP_2$ (*ID*)	$ZnSnP_2$ (*D*)
FP- LAPW	1.135[a]	1.079[a]	0.776[a]
Expt	2.07[b]	2.34 (*D*)[b]	1.66[b]
PVMB approach	1.11[c]	—	0.61[c]
LDA-LMTO	1.22[d]	1.16[d]	—
Expt of *c*-Binary	*c*-AlP	*c*-GaP	*c*-InP
	3.62[e]	2.89[e]	1.42[e]
		3.38[f]	1.37[g]

The notation of the different band gaps are as follows: pseudo-direct: (PD: $\Gamma_{4v} \to \Gamma_{3c}$), direct: (*D*: $\Gamma_{4v} \to \Gamma_{1c}$), indirect: (ID: $\Gamma_{4v} \to T_{1c}+T_{2c}$ for $ZnGeP_2$).
[a]Present work.
[b]Experimental data taken from Ref. [24].
[c]Data taken from Ref. [19].
[d]Data taken from Ref. [23].
[e]Experimental data for the binary analogues taken from Ref. [30].
[f]Experimental data for the binary analogue (*c*-GaP) taken from Ref. [31].
[g]Experimental data for the binary analogue (*c*-InP) taken from Ref. [32].

are given by

$$\varepsilon_2^{ij}(\omega) = \frac{Ve^2}{2\pi\hbar m^2\omega^2}\int d^3k \sum_{nn'}\langle Kn|p_i|Kn'\rangle\langle Kn'|p_j|Kn\rangle \times f_{kn}(1-f_{kn'})\delta(\varepsilon_{kn'}-\varepsilon_{kn}-\hbar\omega) \quad (1)$$

here $(p_x, p_y, p_z) = p$ is the momentum operator, f_{kn} is the Fermi distribution, and $|Kn\rangle$ the crystal wave function, corresponding to energy eigenvalue ε_{kn} with crystal momentum K . The real part of the components of the dielectric function $\varepsilon_1(\omega)$ are then calculated using the Kramer–Kronig transformation. The knowledge of both real and imaginary parts of the dielectric function allows the calculation of important optical constants. In this paper, we present and analyse the reflectivity $R(\omega)$ which is derived from the Fresnel's formula for normal incidence assuming an orientation of the crystal surface parallel and perpendicular to the optical axe using the relation:

$$R(\omega) = \left|\frac{\sqrt{\varepsilon(\omega)}-1}{\sqrt{\varepsilon(\omega)}+1}\right|^2. \quad (2)$$

Due to the tetragonal structure of the chalcopyrite crystals the dielectric function is a tensor [24,39–41], then, we have calculated the two components $E\|c$ and $E\perp c$ of the dielectric function and the reflectivity spectra corresponding to the electric field parallel and perpendicular to the crystallographic axis c. Our calculated static dielectric functions and static refractive indices of these materials are presented in Table 4.

The analysis of the imaginary parts of the dielectric function curves (Fig. 4) of all $ZnSiP_2$, $ZnGeP_2$, and $ZnSnP_2$ semiconductors shows that the spectra can be divided into two major groups of the peaks, the first from 1 eV to 3.5 eV and the second from 3.5 eV to 5 eV. The first group is dominated by Zn–sp transitions, where the first interband transition arises between the upper valence band and the minimum of the conduction band, the first peak is due to the Γ direction of the Brillouin zone is located at the energies near to 2.95 and 2.21 eV for $ZnSiP_2$, and $ZnGeP_2$ respectively, and to 2.24 eV, 2.40 eV for $ZnSnP_2$ in both parallel and perpendicular polarizations ($\varepsilon_{2//}, \varepsilon_{2\perp}$), respectively. The second group of the peaks is deduced from the X-sp transitions (with X = Si for $ZnSiP_2$, Ge for $ZnGeP_2$, and Sn for $ZnSnP_2$), where the main peak is located at 4 eV in all three materials, and mainly arise from the T direction of the Brillouin zone.

Table 4
Static dielectric and static refractive index

	$\varepsilon_\perp$ (0)	$\varepsilon_\|$ (0)	$n_\perp$ (0)	$n_\|$ (0)
$ZnSiP_2$	11.2434	11.3782	33,531	33,731
$ZnGeP_2$	12.5248	12.8059	35,390	35,785
$ZnSnP_2$	12.7513	12.6769	35,709	35,604

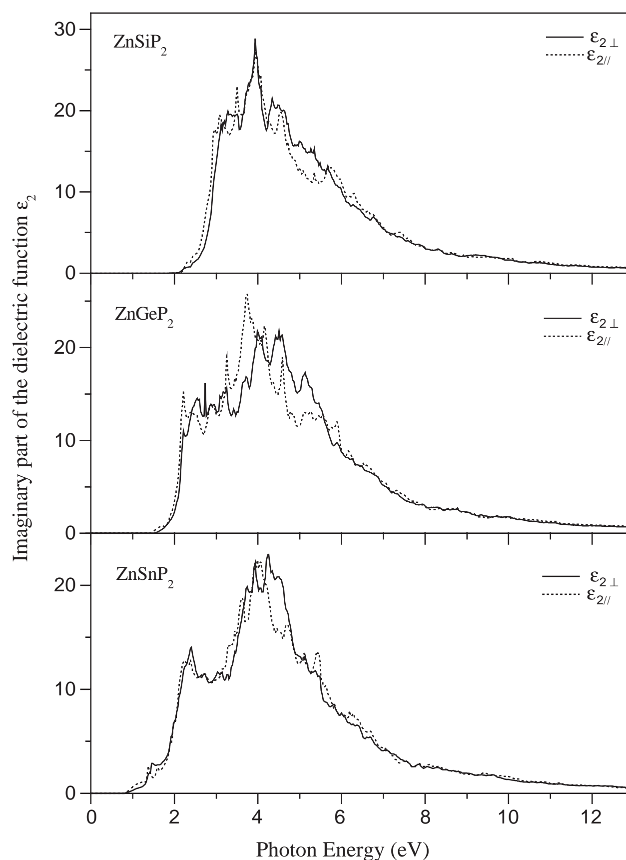

Fig. 4. The imaginary parts of the dielectric function for all $ZnSiP_2$: curve (a), $ZnGeP_2$: curve (b), and $ZnSnP_2$: curve (c).

3.2.1. Fundamental gap transition

For illustrative proposes the model of the generic band structure and selection rules for the transitions in a chalcopyrite crystal [5] are presented in Fig. 5(a, and b). For the direct energy gap like $ZnSnP_2$, the triple degeneracy Γ_{15v} valence band of its c-InP binary analogue (see Fig. 5b) is completely removed in a chalcopyrite crystal due to the simultaneous effects of the non cubic crystalline field and spin orbit interaction, but in absence of this latter, Γ_{15v} splits into a non-degenerate level Γ_{4v} lying above a doubly degenerate Γ_{5v} transition leading to a double transitions, one at $\Gamma_{4v} \rightarrow \Gamma_{1c}$ allowed for the parallel polarization ($E\|c$), and the second at $\Gamma_{5v} \rightarrow \Gamma_{1c}$ allowed for the perpendicular polarization ($E\perp c$). These two transitions are associated to E_0 (A), E_0 (B), respectively and present the fundamental transitions in this compound (see Fig. 5a).

Further more, the restricting of the Brillouin zone for chalcopyrite crystals [5] relative to that for Zinc Blende crystals results in the interesting possibility which have seen in the electronic properties section that the ternary

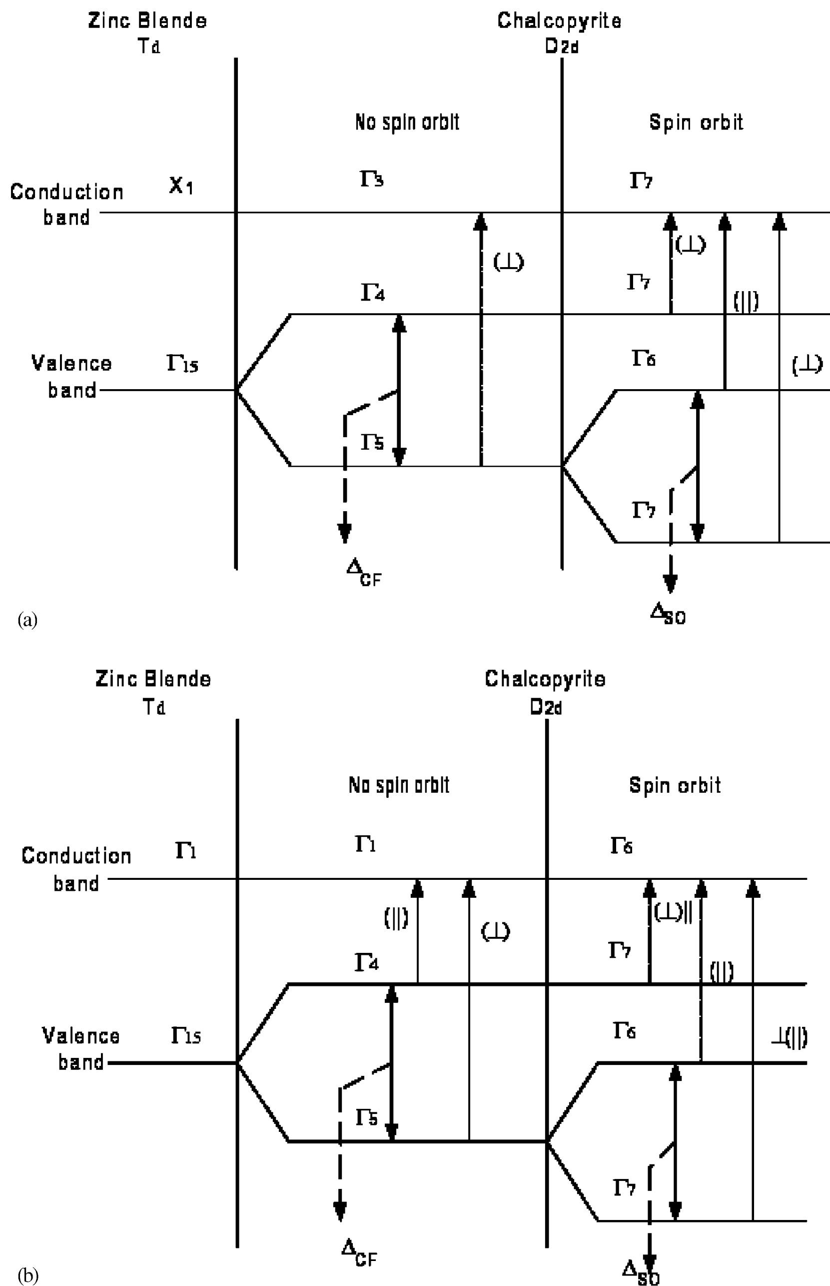

Fig. 5. Generic band structure and selection rules for the transitions in a Chalcopyrite crystal derived from (a): the $\Gamma_{15v} \rightarrow X_{1c}$ indirect transitions and (b): the $\Gamma_{15v} \rightarrow \Gamma_{1c}$ direct transitions in a Zinc Blende crystal.

$ZnSiP_2$ compound have a direct energy gap whereas its *c*-AlP binary analogue have an indirect energy gap. This direct energy gap have been designated as "pseudo-direct", in absence of spin orbit interactions like as in our calculations, the first transition at $\Gamma_{4v}\rightarrow\Gamma_{3c}$ are forbidden altogether, and the second transition at $\Gamma^2_{5v}[\Gamma_{15v}] \rightarrow \Gamma_{3c}[X_{1c}]$ are allowed only for the perpendicular polarization ($E\perp c$) which represent the fundamental transition in this compound (see Fig. 5a) and are the notation of $E(\Gamma X)$. These transitions have been designated as "pseudo-direct" which are correspond to an indirect transition of the binary analogue. Then after the fundamental indirect transition of the $ZnGeP_2$, we have derived the same assignment of the pseudo-direct transition like in $ZnSiP_2$ compound.

3.2.2. *Assignment of the possible optical transitions*

By inspecting both reflectivity spectra which is plotted in Figs. 7(a–c) and the imaginary part of the dielectric function (Figs. 4(a–c)) for $ZnSiP_2$, $ZnGeP_2$ and $ZnSnP_2$, respectively, we can establish a general pattern for the outstanding optical transitions above the fundamental

gap of these materials using the proposed assignments and notation of the main optical transitions in the generic band structure that is displayed in Fig. 6 [41] .

Since, there are two type of transitions, the first one are pseudo-direct transitions, with no corresponding direct transitions in binary analogue, their possible assignments by symmetry are: $E'(\Gamma X) : \Gamma^2_{5v}[\Gamma_{15v}] \rightarrow \Gamma_{2c}[X_{3c}]; E(X\Gamma) : \Gamma^1_{5v}[X_{5v}] \rightarrow \Gamma_{1c}[\Gamma_{1c}]$; (the notation of critical points between brackets denote the transition in binary analogue [41]). Also the structure labelled $E(\Delta X)$ appears in $E \perp c$, and has no corresponding direct transitions in the Zinc Blende structure. The only matching transition from the upper valence band to the conduction band would be the pseudo-direct transition $T_{3v} + T_{4v}[\Delta_{3v} + \Delta_{4v}] \rightarrow T_{1c} + T_{2c}[X_{1c}]$. The second are the direct transitions and are associated to (E_1, E_2)-like transitions which appears into both polarizations (parallel and perpendicular to c axis), they have a direct transitions with respect to the binary analogues, are: $E_1(A) : N^{51}_{1v} \rightarrow N^1_{1c}$, $E_1(B) : N^{52}_{1v} \rightarrow N^1_{1c}$, $E_2(A) : T_{3v} + T_{4v}[X_{5v}] \rightarrow T^1_{5c}[X_{1c}]$, $E_2(B) : T_{5v}[2X_{5v}] \rightarrow T^1_{5c}[X_{1c}]$.

In $ZnSiP_2$ material (Fig. 7a) the first strong transition above the fundamental gap transition called $E_1(A)$ is direct because it allowed in both polarizations($E \perp c$ and $E \| c$) at 2.5 eV, this latter appears after the weaker pseudo-direct transitions $E(\Gamma X)$ and $E'(\Gamma X)$, above it there is a pseudo-direct transition $E(\Delta X)$, and about 2.6 eV there is another strong direct transition $E_1(B)$ that allowed in both polarization, then we observe a group of direct transitions: $E_0(A)$, $E_0(B)$, $E_2(A)$, and $E_2(B)$ located at 2.62–3.5 eV, finally we find the last transition which allowed in $E \perp c$ polarization called $E(X\Gamma)$ at about 5 eV.

Then in $ZnGeP_2$ material (Fig. 7b) the first direct transition above the fundamental gap appear after the

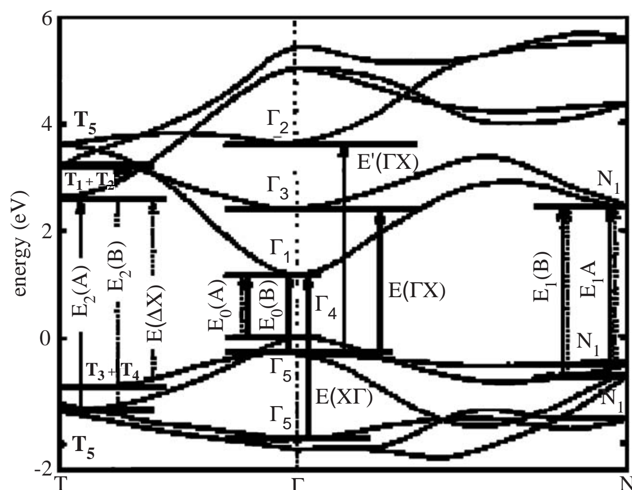

Fig. 6. Assignments of the different interband transitions observed in ternary chalcopyrite semiconductors (figure taken from Ref. [41]).

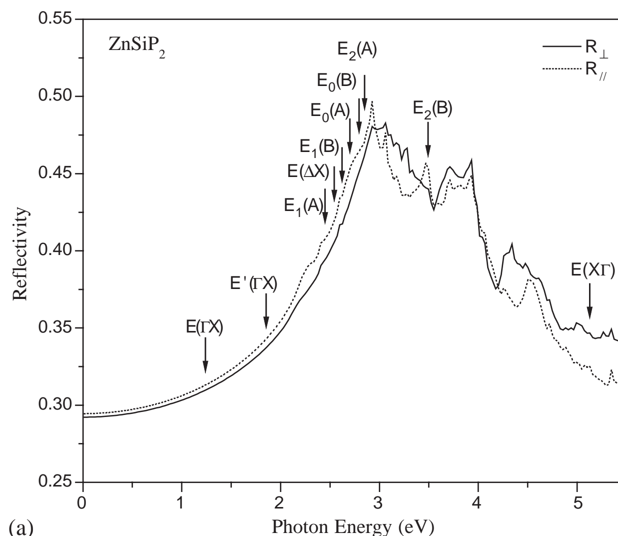

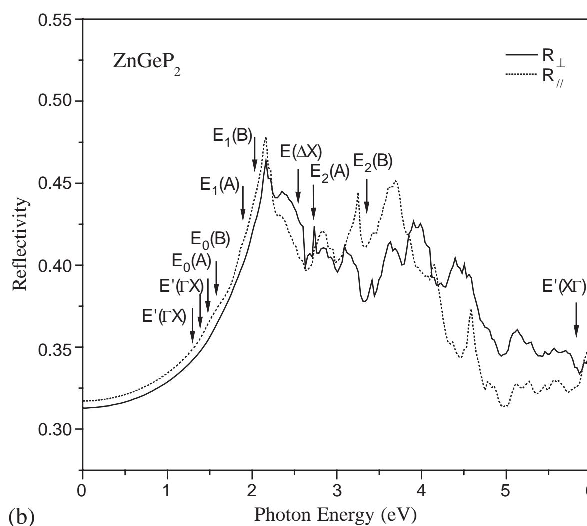

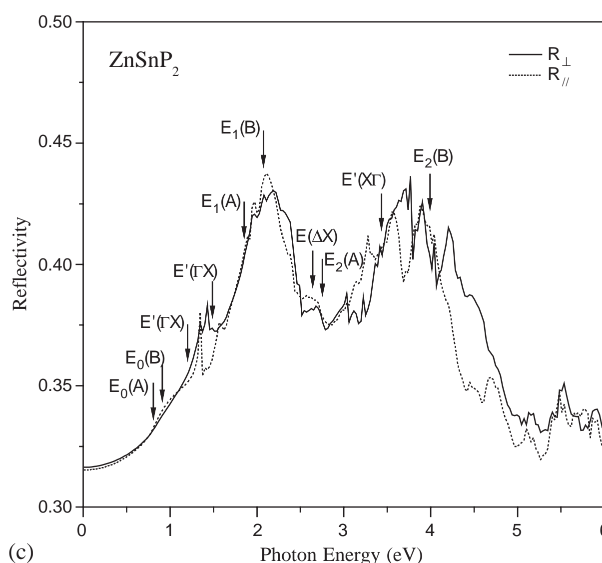

Fig. 7. (a) The reflectivity spectra of the $ZnSiP_2$ semiconductor; (b) the reflectivity spectra of the $ZnGeP_2$ semiconductor; (c) the reflectivity spectra of the $ZnSnP_2$ semiconductor.

Table 5
Main optical transitions energies (in eV) and their correspondence polarizations above the fundamental gap in the band structure

Label	Transition	Major contribution transitions in R			Energy from the band structure		
		$ZnSiP_2$	$ZnGeP_2$	$ZnSnP_2$	$ZnSiP_2$	$ZnGeP_2$	$ZnSnP_2$
$E_0(A)$	$\Gamma_{4v} \rightarrow \Gamma_{1c}$	2.625	1.455	0.802	2.609	1.442	0.776
$E_0(B)$	$\Gamma^1_{5v} \rightarrow \Gamma_{1c}$	2.761	1.537	0.829	2.744	1.523	0.778
$E_1(A)$	$N^{51}_{1v} \rightarrow N^1_{1c}$	2.517	1.945	1.891	2.515	1.942	1.872
$E_1(B)$	$N^{52}_{1v} \rightarrow N^1_{1c}$	2.598	2.081	2.081	2.593	2.057	2.016
$E_2(A)$	$T_{3v} + T_{4v} \rightarrow T^1_{5c}$	2.789	2.789	2.734	2.769	2.744	2.723
$E_2(B)$	$T_{5v} \rightarrow T^1_{5c}$	3.496	3.333	3.959	3.531	3.307	3.938
$E(\Gamma X)$	$\Gamma^1_{5v} \rightarrow \Gamma_{3c}$	1.265	1.265	1.210	1.269	1.258	1.189
$E'(\Gamma X)$	$\Gamma^1_{5v} \rightarrow \Gamma_{2c}$	1.863	1.483	1.483	1.867	1.478	1.464
$E(X\Gamma)$	$\Gamma^2_{5v} \rightarrow \Gamma_{1c}$	5.074	5.836	3.469	5.067	5.811	3.447
$E(\Delta X)$	$T_{3v} + T_{4v} \rightarrow T_{1c} + T_{2c}$	2.571	2.571	2.680	2.558	2.548	2.677

pseudo-direct transition $E(\Gamma X)$, called $E_0(A)$ at 1.4 eV which allowed in both polarizations, above it there is a pseudo-direct transition $E'(\Gamma X)$, and about 1.5 eV there is another direct transition $E_0(B)$, then after these transitions appear a direct strong transitions $E_1(A)$, $E_1(B)$, located at 2 eV, and we observe the two last strong direct transitions $E_2(A)$, $E_2(B)$ after a weaker pseudo-direct transition $E(\Delta X)$, finally we find the transition $E(X\Gamma)$ at about 5 eV which allowed in $E\perp c$ polarization.

While in $ZnSnP_2$ compound the fundamental transition is at $\Gamma_{4v} \rightarrow \Gamma_{1c}$ and represent the direct band gap, the spectra of this compound (Fig. 7c) showed that close to 0.8 eV a double structures is observed: $E_0(A)$ and $E_0(B)$ are allowed in $\perp$ and || polarization's, respectively. Then the next strong direct transitions $E_1(A)$, and $E_1(B)$ are allowed in both polarization ($\perp$ and $\parallel$), and they appear after the weaker pseudo-direct transition $E'(\Gamma X)$at about 2 eV. Nearby, and only in parallel polarization emerges a transition $E(\Delta X)$, located at $\approx$2.7 eV below both $E_2(A)$, and $E_2(B)$ strong direct transitions. All these transitions are presented in Table 5.

4. Conclusion

To conclude, our electronic properties studies using the FAPW+ *lo* method within LDA, suggest that the $ZnSiP_2$ has a pseudo-direct band gap, and the $ZnGeP_2$ has an indirect band gap, then the $ZnSnP_2$ has a direct energy gap. In the important section, we have studied the optical properties where we have determined the real and imaginary parts of the dielectric function, and we have presented the assignment of the optical transitions with respect to their representation in a reflectivity spectra compared to the electronic band structure, the analysis of these curves show that the ternary Pnictides semiconductors $ZnSiP_2$, $ZnGeP_2$, and $ZnSnP_2$ have two type of transitions: direct transitions which correspond to a like direct transitions in the Zinc Blende binary analogues, these transitions are strong and they appear in both polarizations ($E\perp c$ and $E\parallel c$), where the second type of transitions are the pseudo-direct which correspond to an indirect transitions in their binary analogues, and they are weaker because they appear in one polarization ($E\perp c$ or $E\parallel c$).

Acknowledgments

This work was supported in part by the Algerian–-French Ministries of Foreign Affairs under project CMEP 02 MDU 546. The authors are grateful to CCML (Lens, France) for the technical support found in visiting the center.

References

[1] M.C. Ohmer, R. Pandey, Mater. Res. Bull. 23 (1998) 16.
[2] S.N. Rashkeev, S. Limpijumnong, W.R.L. Lambrecht, Phys. Rev. B 59 (1999) 2737.
[3] H.M. Hobgood, T. Henningsen, R.N. Thomas, R.H. Hopkins, M.G. Ohmer, W.C. Mitchel, D.W. Fischer, S.M. Hegde, F.K. Hopkins, J. Appl. Phys. 73 (1993) 4680.
[4] G.G. Xing, K. J. Bachmenn, J. B. Posthill, M. L. Timmons, in: J. T. Glass, R. Messier, N. Fujimori (Eds.), Diamond, Silicon Nitride, and Related Wide Band Gap Semiconductors, MRS, Symposia Proceedings No. 162, Materials Research Society, Pittsburg, 1989, p. 651, and references therein.
[5] R. A. Mickelsen, W. S. Chen, in: Proceedings of the 15th IEEE Photovoltaic Specialists Conference 1981, IEEE, New York, 1981, p. 800. Available as IEEE Publ. 81 CH 1644-4.
[6] N. Yamamoto, Jpn. J. Appl. Suppl. 19 (1980) 95.
[7] W.E. Devaney, R.A. Mickelsen, W.S. Chen, in: Proceedings of the 18th IEEE Photovoltaic Specialists Conference, Las Vegas, NV, 1985, p. 1733.

[8] J. Loferski, J. Sewchum, B. Roesler, R. Beaulieu, J. Pleskoszeski, M. Gorska, G. Chapman, in: Proceedings of the 13th IEEE Photovoltaic Specialists Conference, 1978, p. 190.
[9] W. Kohn, L.J. Sham, Phys. Rev. A 140 (1965) 1133.
[10] P. Hohenberg, W. Kohn, Phys. Rev. B 136 (1964) 864.
[11] J.C. Slater, Phys. Rev. 51 (1937) 846;
T.L. Loucks, Augmented Plane Wave Method, W.A. Benjamin Inc., New York, 1967.
[12] J. Korringa, Physica 13 (1947) 392;
W. Kohn, N. Rostoker, Phys. Rev. 94 (1954) 1111.
[13] O.K. Andersen, Phys. Rev. B 12 (1975) 3060.
[14] E. Sjöstedt, L. Nordström, D.J. Singh, Solid. State. Commun. 114 (2000) 15.
[15] K. Schwarz, P. Blaha, G.K.H. Madsen, Comput. Phys. Commun. 147 (2002) 71.
[16] F. Chiker, B. Abbar, A. Tadjer, S. Bresson, B. Khelifa, C. Mathieu, Phys. B: Phys. Condens. Matter 349/1–4 (2004) 181.
[17] J.P. Perdew, Y. Wang, Phys. Rev. B 45 (1992) 13244.
[18] J.A. Van Vechten, Phys. Rev. 182 (1969) 891.
[19] J.A. Van Vechten, Phys. Rev. B 1 (1970) 3351.
[20] J.C. Philips, Rev. Mod. Phys. 42 (1970) 317.
[21] D.S. Chemla, Phys. Rev. 23 (1971) 1441.
[22] B.F. Levine, Phys. Rev. B 7 (1973) 2591.
[23] B.F. Levine, J. Chem. Phys. 59 (1973) 1463.
[24] J.L. Shay, J.H. Wernick, Ternary Chalcopyrite Semiconductors: Growth, Electronic Properties and Applications, Pergamon Press, Oxford, 1975.
[25] H. Matsusita, S. Endo, T. Irje, Jpn. J. Appl. Phys. 30 (1991) 1181.
[26] J.E. Jaffe, A. Zunger, Phys. Rev. B 29 (1984) 1882.
[27] J.E. Jaffe, A. Zunger, Phys. Rev. B 30 (1984) 741.
[28] V. Kumar, D. Chandra, Phys. Stat. Sol. (B) 212 (1992) 282.
[29] V. Kumar, J. Phys. Chem. Solids. 61 (2000) 91.
[30] X. Zhu, S.G. Louie, Phys. Rev. B 43 (1991) 14142;
S. Massida, A. Continenza, A.J. Freeman, T.M. De. Pascale, F. Meloni, M. Serra, Phys. Rev. B 41 (1990) 12079.
[31] P.J. Dean, D.G. Thomas, Phys. Rev. 150 (1966) 690.
[32] M. Cardona, K.L. Shaklee, F.H. Pollak, Phys. Rev. 154 (1967) 696.
[33] J.L. Shay, B. Tell, E. Buehler, J.H. Wernick, Phys. Rev. Lett. 14 (1973) 983.
[34] J.E. Jaffe, A. Zunger, Phys. Rev. B 30 (1984) 741.
[35] C. Varea De alvarez, M.L. Cohen, Phys. Rev. Lett. 30 (1973) 979.
[36] C. Varea De alvarez, M.L. Cohen, S.E. Kohn, Y. Petroff, Y.R. Shen, Phys. Rev. B 10 (1974) 5175.
[37] S. Limpijumnong, W.R.L. Lambrecht, B. Segall, Phys. Rev. B 60 (1999) 8087.
[38] P. Zapol, Ph. D. Theis, Michigan Technological University, 1998. Avail. UMI Order No. DA9823065.
[39] F. Chiker, B. Abbar, A. Tadjer, H. Aourag, B. Khelifa, J. Mater. Sci. Eng. B 98 (2002) 81.
[40] F. Chiker, B. Abbar, H. Aourag, A. Tadjer, S. Bresson, B. Khelifa, C. Mathieu, Chem. Phys. 298 (2004) 135–140.
[41] M.I. Alonso, K. Wakita, J. Pascual, M. Garriga, N. Yamamoto, Phys. Rev. B 63 (2001) 075203.